Science of the Total Environment 633 (2018) 452–462

Contents lists available at ScienceDirect

Science of the Total Environment

journal homepage: www.elsevier.com/locate/scitotenv

Temporal and spatial variations in sand and dust storm events in East Asia from 2007 to 2016: Relationships with surface conditions and climate change

Linchang An [a,b,c], Huizheng Che [a,*], Min Xue [a], Tianhang Zhang [c], Hong Wang [a], Yaqiang Wang [a], Chunhong Zhou [a], Hujia Zhao [a], Ke Gui [a,b], Yu Zheng [a,d], Tianze Sun [a,b], Yuanxin Liang [a,b], Enwei Sun [d], Hengde Zhang [c], Xiaoye Zhang [a]

[a] Key Laboratory of Atmospheric Chemistry of CMA, Institute of Atmospheric Composition, Chinese Academy of Meteorological Sciences, Beijing 100081, China
[b] College of Earth Science, University of Chinese Academy of Sciences, Beijing 100081, China
[c] National Meteorological Center, CMA, Beijing 100081, China
[d] Nanjing University of Information Science & Technology, Nanjing 210044, China

HIGHLIGHTS

- Sand and dust storms in East Asia (2006–2017) weakened significantly.
- Increasing vegetation cover in the dust source area control the soil degradation.
- Polar vortex indirectly affects sand and dust storms by reducing the wind speed.

GRAPHICAL ABSTRACT

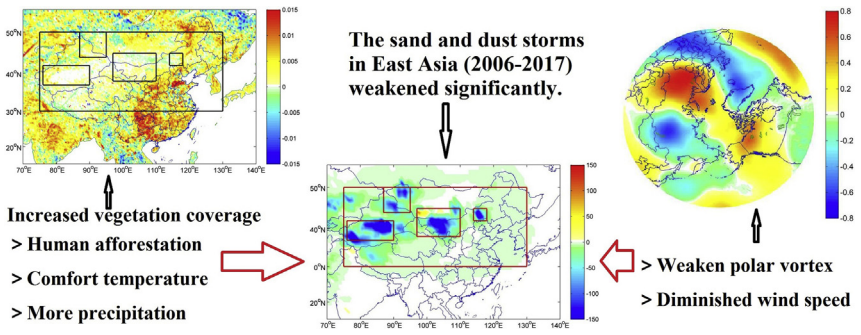
The sand and dust storms in East Asia (2006-2017) weakened significantly.
Increased vegetation coverage
> Human afforestation
> Comfort temperature
> More precipitation
> Weaken polar vortex
> Diminished wind speed

ARTICLE INFO

Article history:
Received 5 January 2018
Received in revised form 6 March 2018
Accepted 7 March 2018
Available online 28 March 2018

Editor: Jianmin Chen

Keywords:
Sand and dust storms
Surface conditions
NDVI
Climate change

ABSTRACT

We analyzed the frequency and intensity of sand and dust storms (SDSs) in East Asia from 2007 to 2016 using observational data from ground stations, numerical modeling, and vegetation indices obtained from both satellite and reanalysis data. The relationships of SDSs with surface conditions and the synoptic circulation pattern were also analyzed. The statistical analyses demonstrated that the number and intensity of SDS events recorded in spring during 2007 to 2016 showed a decreasing trend. The total number of spring SDSs decreased from at least ten events per year before 2011 to less than ten events per year after 2011. The overall average annual variation of the surface dust concentration in the main dust source regions decreased 33.24 μg/m^3 (−1.75%) annually. The variation in the temperatures near and below the ground surface and the amount of precipitation and soil moisture all favored an improvement in vegetation coverage, which reduced the intensity and frequency of SDSs. The strong winds accompanying the influx of cold air from high latitudes showed a decreasing trend, leading to a decrease in the number of SDSs and playing a key role in the decadal decrease of SDSs. The decrease in the intensity of the polar vortex during study period was closely related to the decrease in the intensity and frequency of SDSs.

© 2018 Elsevier B.V. All rights reserved.

* Corresponding author.
E-mail address: chehz@cma.gov.cn (H. Che).

https://doi.org/10.1016/j.scitotenv.2018.03.068
0048-9697/© 2018 Elsevier B.V. All rights reserved.

1. Introduction

Sand and dust storms (SDSs) are natural events that can have disastrous effects on both the environment and human activities (Sun et al., 2001; Zhou and Wang, 2002; Tam et al., 2012). SDS events in East Asia mainly occur in the spring and may cause a decrease in visibility to <10 km, or even occasionally to <0.1 km. The concentrations of particles with diameters <10 μm increase significantly, which affects the air quality and can cause respiratory symptoms in humans (Zhang et al., 1998; Kim et al., 2001; Seinfeld et al., 2004; Che et al., 2006; Meng and Lu, 2007). The sand and dust particles influence weather systems and the climate by changing the radiation balance, both directly by absorbing and scattering radiation and indirectly by affecting the cloud cover when they act as cloud condensation nuclei (Tegen, 2003; Gong et al., 2006; Che et al., 2013; Bi et al., 2014; Huang et al., 2014; Che et al., 2015). In addition, Essential micronutrients are carried to the oceans by these sand and dust particles, providing nutrients via processes such as particle floating, adsorption and co-precipitation (Yuan and Zhang, 2006; Wang et al., 2009; Martínez-Garcia et al., 2011; Tan et al., 2012; Tan et al., 2013; Fan et al., 2017).

There have been many studies of the distribution and frequency of SDSs in East Asia in recent years. Ground observation records, satellite data, and dust model results are used to analyze the distribution and frequency of SDSs in East Asia (Zhang et al., 2003a; Mikami et al., 2005; Xu et al., 2011; Li et al., 2012; Chen et al., 2017a). In particular, an integrated SDSs forecasting system–CUACE/Dust (Chinese Unified Atmospheric Chemistry Environment for Dust) has been developed and successfully used in the SDSs forecasts in East Asia (Gong and Zhang, 2008). The main source areas for dust in East Asia are the deserts and semiarid regions of Mongolia and northern China (Wang et al., 2006; Wang et al., 2008a), from where ~800 Tg of sand and dust particles are injected into the atmosphere annually. About 30% of these particles are redeposited in the desert regions and about 70% left the source areas and are transported to North China, the Korean Peninsula, Japan, and the northern Pacific Ocean, with some particles even reaching America and France (Zhang et al., 1997; Chun et al., 2001; Zhang et al., 2003b; Grousset et al., 2003; Mukai et al., 2004; Che et al., 2005; Yuan and Zhang, 2006; Gong et al., 2007; Zhang et al., 2008). There are two main reasons for the variation in the distribution and frequency of SDSs in East Asia directly: (1) changes in the surface conditions of the source areas and (2) variations in the wind in the near-surface layer (Zhang et al., 2005; Yu et al., 2009). Both of these reasons are closely related to climate change. Precipitation, soil moisture, low air temperature, surface soil conditions as well as human activities are the important factors that determine the vegetation coverage and then influence SDSs events indirectly (Natsagdorj et al., 2003;Liu et al., 2004; Lee and Sohn, 2011; Wang et al., 2018). Furthermore, the distribution and frequency of SDSs are strongly related to the near-surface wind which is supposed to be linked with large-scale atmospheric circulations such as polar vortex, cold air activity, surface pressure field, and so on (Littmann, 1991; Qian et al., 2002; Zhao et al., 2004; Yang et al., 2007).

Although many studies have been conducted, there is still a lack of high-quality dust data with excellent temporal and spatial resolution. The ground observation data lack long-term continuous dust concentration records, and the spatial resolution of the observation station also restricts studies. The satellite observation data and mode simulation results have good temporal and spatial resolution, and there are large quantities of algorithm researches (Qu et al., 2006; Chen et al., 2017a, 2017b), the accuracy of data still needs to be improved. Most previous studies tend to focus only on the ground condition, or studies only on the climate facts. It still needs comprehension to analyze the factors related to SDSs. Although considerable research has been devoted to study the increase of SDSs events, few attention has been paid to the reasons why SDSs weakened significantly in recent years.

Therefore, this paper intends to make a comprehensive study of the reduction of the distribution and frequency of SDSs in East Asia in recent years, by using both ground observation data and dust model results in order to get better spatial and temporal resolution and accuracy. We carried out a detailed analysis of the distribution and frequency of SDSs in East Asia from 2007 to 2016. The relationship between the variation in climatic factors (such as temperature, air pressure, wind, polar vortex, and so on) and the occurrence of SDSs were compared to determine the main controls on the interannual variation in SDSs. This research may provide scientific support for the prevention and mitigation of SDSs in East Asia.

2. Materials and methods

2.1. Observational data from ground stations

The China Meteorological Administration (CMA) grades the weather phenomenon of SDSs into five levels: floating dust; blowing dust; SDSs; severe SDSs; and super-severe SDSs. The near-surface wind speed and the horizontal visibility are used to characterize this weather phenomenon when winds blow dust or sand up from the ground (Table 1).

Based on records from 673 standard ground stations in China (Fig. 1), we recorded three grades of sand and dust event: Blowing Sand or Dust (BSD); SDS; and severe SDS. BSD is recorded when at least five adjacent standard ground stations record blowing dust or a more severe sand and dust phenomena at the same observation time during a sand and dust event. An SDS event is recorded when at least three adjacent standard stations record an SDS or a more severe sand and dust phenomena at the same observation time in a sand and dust event. A severe SDS process is recorded when at least three adjacent standard stations record a severe SDS or a more severe sand and dust phenomena at the same observation time in a sand and dust event. If a sand and dust event meets two or three of these conditions, the most severe grade will be recorded (CMA, 2006). BSD is named and recorded as weaker than an SDS event as a result of the low visibility. Therefore we described three grades of sand and dust event as SDSs.

2.2. Surface dust concentration of CUACE/Dust model

The Chinese Unified Atmospheric Chemistry Environment for Dust (CUACE/Dust) is an operational mesoscale numerical model to forecast SDSs in East Asia. The model includes a comprehensive dust aerosol module with emission, dry/wet deposition, and other dynamic atmospheric processes. CUACE/Dust combines observational data from the CMA ground dust monitoring network and retrieves dust information from Chinese geostationary satellites in a data assimilation system (Gong and Zhang, 2008; Wang et al., 2008b). A threat score system evaluated the performance of CUACE/Dust against all available observations in 2006 and gave an average threat score in spring of 0.31 for 24 h forecasts, 0.23 for 48 h forecasts, and 0.21 for 72 h forecasts (Zhou et al., 2008). CUACE/Dust operations began in 2007 and we assessed the model using the surface dust concentration product over 119 SDS events occurring during 2007 and 2016. The results showed that the

Table 1
Wind speed and visibility in sand and dust weather phenomena.

	Floating dust	Blowing dust	SDS	Severe SDS	Super-severe SDS
Wind speed (m/s)	≤3.0	>3.0	>3.0	>3.0	>3.0
Visibility (km)	<10	1–10	0.5–1	0.050–0.5	<0.050

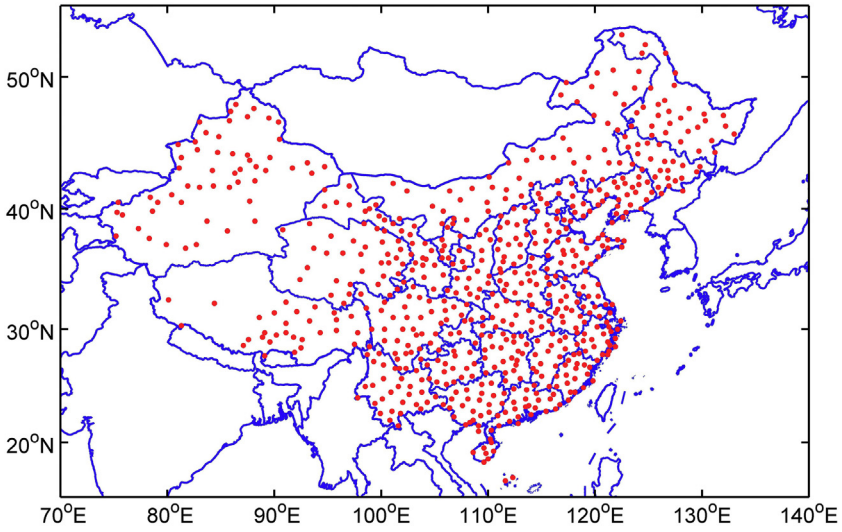

Fig. 1. Locations of the 673 standard ground weather stations in China.

average threat score for 24 h forecasts was 0.31 (Table 2), suggesting that the 24 h surface dust concentration is highly accurate. The domain of CUACE/Dust mode in this study is 70°E~140°E, 15°N~55°N to cover east Asia,with a dimension of 81 × 141 and a resolution of 54 km (~0.5°).

2.3. Normalized Difference Vegetation Index data

The Normalized Difference Vegetation Index (NDVI) data from the Moderate Resolution Imaging Spectroradiometer (MODIS) is a vegetation index determined by blue, red, and near-infrared reflectance centered at 469, 645, and 858 nm, respectively (Didan, 2015). The NDVI is used to monitor and display global monitoring data for the condition of vegetation and land cover. MODIS NDVI data can be used to characterize biological properties and processes at the Earth's surface, including primary production and changes in land cover. The MODIS NDVI data have a close negative relationship with the distribution and frequency of SDSs. NDVI values <0 indicate areas covered by water, snow, or tjaele. Areas where the NDVI is <0.15–0.2 (the threshold value varies with the surface condition) are considered to be prone to erosion, and areas with higher NDVI indicate higher green leaf coverage which means a better vegetation coverage (Miller et al., 2006; Kim et al., 2013; Tan and Li, 2015).

The monthly average MODIS NDVI composite grid data (MOD13A3) at 0.01° (~1 km) resolution were obtained from the National Aeronautics and Space Administration. The MOD13A3 product data were computed from atmospherically corrected bi-directional surface reflectance data that had been masked for water, clouds, heavy aerosols, and cloud shadows, which absorb all the 16-day 1-km products. The weighted temporal average method was used when the atmosphere was clear and the maximum value was used under cloudy conditions. The compositing process and quality assessment document for the MODIS NDVI are available on the MODIS web site.

2.4. FNL (Final) Operational Model Global Tropospheric Analyses data

The 1° × 1° FNL Operational Model Global Tropospheric Analyses data from the National Centers for Environmental Prediction–National Center for Atmospheric Research (NCEP–NCAR) were acquired from the NCEP–NCAR web site (NCEP, 2000). The data are available at 6 h intervals (00:00 h, 06:00 h, 12:00 h, and 18:00 h UTM). The product was obtained from the Global Data Assimilation System and other sources. The datasets used included the air temperature at 2 m above the ground, the soil temperature 0–0.1 m below the ground, the volumetric soil moisture content 0–0.1 m below the ground, the pressure reduced to mean sea-level, the geopotential height at 500 mbar, the horizontal wind at 850 mbar, and the vertical wind at 850 mbar. The datasets were averaged by month to give an average value in each spring.

2.5. Combined precipitation dataset

Monthly average values for precipitation are available directly from the Global Precipitation Climatology Project (Adler et al., 2003). The data are reported with a 2.5° latitude–longitude geographical resolution. The monthly average precipitation values were averaged to give the average precipitation in the target areas. The Global Precipitation Climatology Project monthly product provides a consistent analysis of global precipitation from an integration of various satellite datasets over land and the oceans and a gage analysis over land. Data from rain gage stations, satellites, and sounding observations were merged to estimate the monthly rainfall on a 2.5° global grid.

3. Results and discussion

A total of 119 SDS events occurred in China during 2007 to 2016, of which 95 (~80%) occurred in spring (March, April, and May). Many previous studies have reported that most dust storms in East Asia occur in

Table 2
Threat scores of CUACE/Dust in sand and dust events from 2007 to 2016.

	2007	2008	2009	2010	2011	2012	2013	2014	2015	2016	Mean
No. of events	18	13	10	18	8	10	10	7	15	10	11.9
24 h forecast	0.27	0.28	0.29	0.31	0.32	0.29	0.30	0.23	0.37	0.41	0.31
48 h forecast	0.24	0.21	0.25	0.25	0.28	0.31	0.21	0.31	0.28	0.35	0.27
72 h forecast	0.27	0.18	0.16	0.21	0.23	0.19	0.19	0.19	0.25	0.26	0.21

Table 3
Number of spring SDS events in China from 2007 to 2016.

	2007	2008	2009	2010	2011	2012	2013	2014	2015	2016	Mean
BSD	5	1	2	8	5	4	5	4	10	5	4.9
SDS	8	8	5	6	1	2	1	1	1	2	3.5
Severe SDS	1	1	0	1	2	2	0	2	1	1	1.1
Total	14	10	7	15	8	8	6	7	12	8	9.5

spring (Yang et al., 2008; Che et al., 2011; Guan et al., 2015; Song et al., 2016) and we therefore focused on SDS events in this season.

3.1. Frequency and distribution of SDSs

We analyzed the frequency of spring SDSs events from 2007 to 2016 based on data from 673 standard ground stations in China. The average number of BSD events in spring during 2007 to 2016 was 4.9, with four or five BSD events in more than half of these years. The number of BSD events in spring 2008 and 2009 was only one and two, respectively, whereas ten events occurred in 2015. Eight SDS events occurred in spring 2007 and spring 2008 and five and six SDS events occurred in 2009 and 2010, respectively. The number of SDS events has fallen sharply to one or two per year since 2011 and the trend of the decrease is clear. Severe SDS events occurred once or twice per year in most of the ten years, although there was no severe SDS event in 2009 and 2013. The number of SDS events showed decreasing trend, meanwhile, that of the BSD events show an increasing trend, indicating the intensity SDSs became weaker.

The average annual number of total SDSs events in spring was 9.5 and there was a gradual decrease in total SDSs events each year. The total number of all SDS events in spring was more than ten (seven in 2009) from 2007 to 2010, whereas between 2011 and 2016 the number was less than ten (12 in 2015). The highest number of all SDSs events (15) occurred in spring 2010 and the second highest number (14) occurred in 2007. There were twice as many SDSs events in spring 2007 than in spring 2013, making 2007 the strongest year for SDSs events, whereas most SDSs events occurred in 2010. Six total SDSs events occurred in spring 2013, the lowest number in the decade under consideration, and the intensity of the SDS events was also the weakest in this year. The number of spring SDS events decreased and the intensity of SDSs became weaker over the time period studied (Table 3).

The distribution of surface dust concentration is an important index of the range and intensity of SDSs. The results of the CUACE/Dust model were processed to give the mean surface dust concentration in each spring. Fig. 2a shows the distribution of the mean surface dust concentration in spring from 2007 to 2016. A high surface dust concentration covers northern China, Mongolia, the Korean Peninsula, and parts of Japan. This area (30–50° N, 75–130° E) has been demarcated as the main dust influence area (MDIA) in East Asia. There are four regions in the MDIA with a particularly high mean surface dust concentration: the southern basin of Xinjiang province (37–42° N, 76–90° E); northeastern Xinjiang and western Mongolia (44–50° N, 87–95° E); western Inner Mongolia and southern Mongolia (38–45° N, 97–110° E); and the center of Inner Mongolia (42–45° N, 114–118° E). These four regions are desert areas (the Gobi Desert or other major sources of dust) and are sequentially defined as regions 1, 2, 3, and 4. Based on the mean surface dust concentration in each spring during study period, the annual mean surface dust concentrations of each grid for the ten-year period were fitted to determine the annual mean variation. The results indicated that the mean surface dust concentration of almost all the MDIA has decreased (Fig. 2b).

The mean surface dust concentration of the MDIA in spring from 2007 to 2016 was 102.66 μg/m^3 and the mean surface dust concentration of the MDIA decreased by 9.9 g/m3 (9.64%) per year. Region 1 had the highest mean surface dust concentration (686.25 μg/m^3), whereas the mean surface dust concentration in regions 2, 3 and 4 were all larger than 200 μg/m^3. The overall average annual variation of the surface dust concentration in the four regions was −33.24 μg/m^3 (−11.75%) per year. The decrease was highest in region 4, where the mean surface dust concentration decreased by 45.05 μg/m^3 (16.25%) per year (Table 4).

3.2. Surface conditions

Western and northern China and western and southern Mongolia have large areas of desert and soil degradation with a spring NDVI <0.2 during 2007 to 2016 (Fig. 3a). These regions were considered to be the main source of dust emissions. Region 1 covered the largest desert region of China, including the Taklimakan Desert, with little vegetation coverage and the mean spring NDVI in this region was 0.067. Regions 2 and 3 were also arid desert regions, including the Gobi Desert, and the mean spring NDVI was about 0.1. Region 4 had a richer vegetation coverage than the other main dust source areas with a mean value of 0.203. There are many other sources of dust in the MDIA, including semiarid areas and unimproved farmland. The mean spring NDVI of the MDIA was 0.247, suggesting a very poor vegetation coverage.

The annual mean variation of the NDVI in most of East Asia was positive, indicating that vegetation coverage has improved and dust emissions have been suppressed in the source areas (Fig. 3b). Areas with a

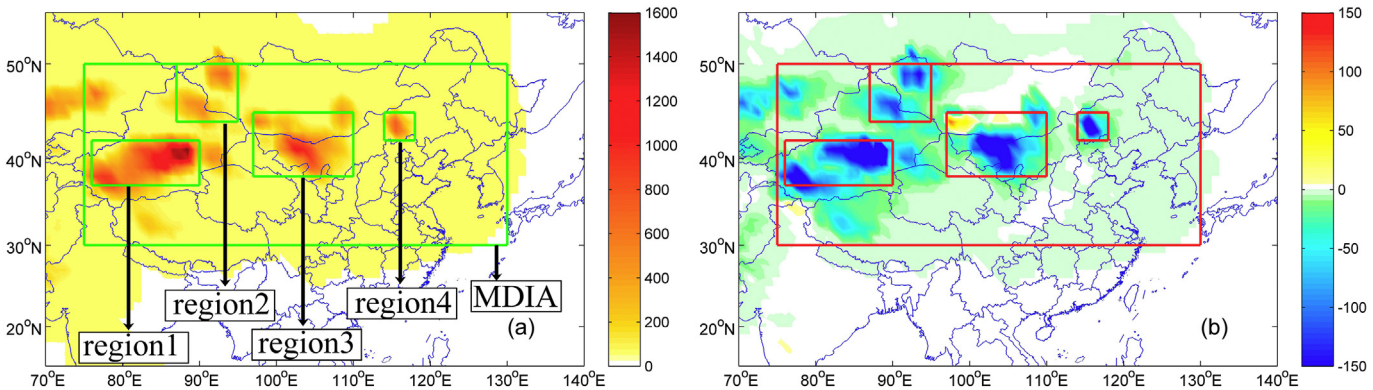

Fig. 2. (a) Mean surface dust concentration and (b) annual mean variation in spring, 2007–2016. Units: μg/m^3.

Table 4
Mean surface dust concentrations, annual mean variations, and rate of the annual mean variations of regions 1–4 in spring (2007–2016).

	MDIA in East Asia	Region 1	Region 2	Region 3	Region 4	Average (regions 1–4)
MSDC (μg/m^3)	102.66	686.25	201.12	259.10	277.20	355.92
Annual mean variation (μg/m^3)	−9.90	−26.85	−29.34	−31.71	−45.05	−33.24
Rate of annual mean variation (%)	−9.64	−3.91	−14.59	−12.24	−16.25	−11.75

higher mean NDVI may show greater improvements in vegetation coverage. The annual mean variation of the NDVI in regions 1, 2 and 3 was 0.0005–0.0006 per year, whereas it was 0.0013 in region 4. The average of the mean rate of annual variation of the four regions was 0.647%, less than the average for the MDIA (0.812). The overall average annual variation of the four regions was 0.647%, less than those for the MDIA (0.812) (Table 5).

There are two main reasons for the improvement in the condition of vegetation coverage: artificial afforestation and climate change (Kelly and Goulden, 2008; Gottfried et al., 2012). To protect the natural environment, many countries have been planting trees and returning farmland to forests. Many measures have been taken at the edge of deserts in China to prevent and control desertification. China's afforestation has increased the forest area by 14 ha per year during the last 2 decades. The area of planted forest in China is ~62 million hectares in 2008, which is the largest in the world (Peng et al., 2014). These activities have effectively prevented soil degradation and the expansion of deserts. However, these measures are unable to change the condition of vegetation coverage in the interior of deserts, including the Gobi Desert. Climate change has also influenced on the condition of vegetation coverage in East Asia, higher surface air and soil temperatures, more precipitation, and a higher soil moisture content during spring now are favorable to plant growth, both on the edge of deserts and in the desert interiors.

The mean spring 2 m temperature in the MDIA varied from −10 to 15° from 2007 to 2016 (Fig. 4a) and soil temperature at 0–0.1 m depth were slightly higher (Fig. 4b). Several degrees of warming both the temperature at 2 m height and the soil temperature at 0–0.1 m depth favor the growth of most plants, which can reduce the incidence of SDSs. However, a higher temperature of the surface air and soil favors atmospheric instability and a vertical upflow of air may exacerbate dust emissions and cause SDSs. The mean spring 2 m temperature in the MDIA was 1.022 °C. Regions 2 and 4 had mean spring 2 m temperature of 1.935 and 1.770 °C, respectively. The mean spring 2 m temperature in regions 1 and 3 were significantly higher (8.550 and 5.030 °C) as a result of the large areas of desert, which ascribed to the higher specific heat capacity for soil dust particles. The mean soil temperature at 0–0.1 m depth had almost the same variation in distribution as the mean spring 2 m temperature.

The annual mean variation in the temperature at 2 m height in most of the MDIA was positive, indicative of the increasing trend of temperature in the near-surface layer (Fig. 4b). The annual increase soil temperature at 0–0.1 m depth in the most of the MDIA was significantly higher than that of the temperature at 2 m height (Fig. 4d). The annual mean variation in the temperature at 2 m height in the MDIA was 0.049°C per year and the variation at 0–0.1 m depth was 0.237 °C per year. The values were higher in regions 1, 2, 3, and 4. The average annual mean variation in temperature at 2 m height in regions 1, 2, 3, and 4 was 0.133 °C per year, whereas the average annual mean variation in soil temperature at 0–0.1 m depth was 0.376 °C per year (Table 5). The changes in temperature of the surface air and soil were also affected by the variation in the meridional wind.

Most of the MDIA has extremely low precipitation in spring, resulting in a severe shortage of water for plant growth. The mean daily precipitation in northern China and Mongolia is much lower than other parts of East Asia (Fig. 5a). The mean daily spring precipitation in the MDIA from 2007 to 2016 was 1.170 mm/day, whereas the precipitation in regions 1, 2, and 4 was 0.5–0.7 mm/day and the precipitation in region 3 was 0.252 mm/day. The annual mean variation in the daily precipitation in the MDIA was 0.018 mm/day per year (1.527%), whereas the variations in regions 1, 2 and 3 were larger than 0, indicating that precipitation exhibited an increasing trend, improving the coverage of vegetation (Fig. 5b). The annual mean variation in daily precipitation in region 4 was −0.020 mm/day per year (−3.969%), which was unfavorable for the coverage of vegetation. However, the annual mean variation of NDVI in region 4 was twofold greater than that in other regions. This may due to the high degree of artificial afforestation; the forests in this area protect the densely populated and highly developed region of eastern China.

The volumetric soil moisture content (VSMC) has a more direct influence on vegetation coverage. The mean VSMC at 0–0.1 m depth in most parts of the MDIA during spring from 2007 to 2016 was <30% (Fig. 6a), which results in the poor growth of vegetation. However, the annual mean variation of the VSMC at 0–0.1 m depth in the MDIA has increased over time (Fig. 6b). The mean VSMC at 0–0.1 m depth in the MDIA was 27.524%, whereas in regions 1–4 the mean values were all <25% and the average of the mean VSMC at 0–0.1 m depth in regions 1–4 was 20.306. Although the yearly increase in precipitation in region l was greater than in other regions, the annual mean variation of the VSMC at 0–0.1 m depth (0.244) was less than in other regions. This may be because the increase in ground temperature resulted in greater evaporation. The annual mean variation of the VSMC at 0–0.1 m depth

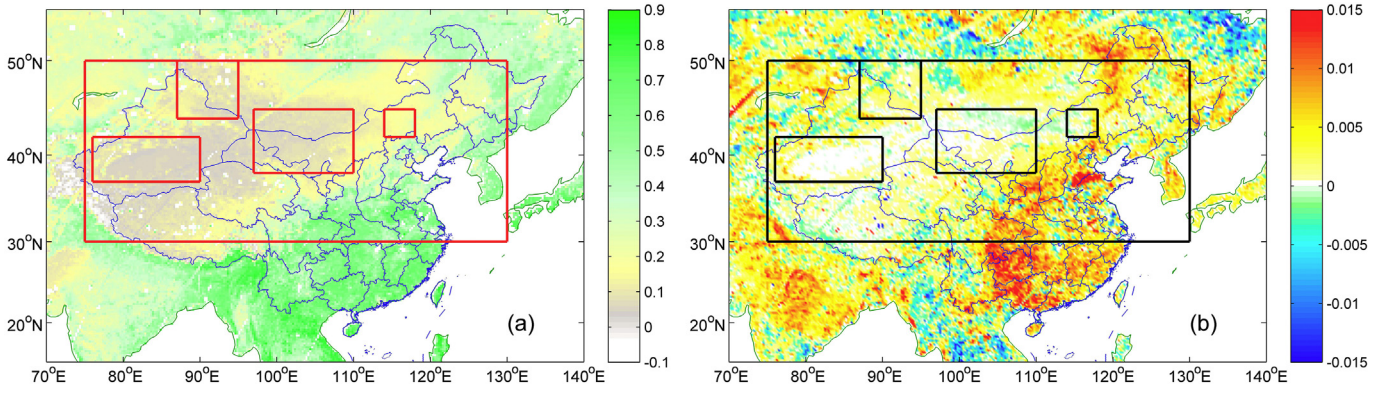

Fig. 3. (a) Mean spring NDVI and (b) annual mean variation of the NDVI in spring (2007–2016).

Table 5
Mean surface factors and annual mean variations (rates) for the major regions in spring (2007–2016).

	MDIA	Region 1	Region 2	Region 3	Region 4	Average (regions 1–4)
Mean NDVI	0.247	0.067	0.102	0.098	0.203	0.118
Annual mean variation	0.0020	0.0005	0.0006	0.0006	0.0013	0.0007
Annual mean variation rate (%)	0.812	0.773	0.587	0.598	0.630	0.647
Mean temperature at 2 m above ground (°C)	1.022	8.550	1.935	5.030	1.770	4.321
Annual mean variation (°C)	0.049	0.118	0.069	0.177	0.169	0.133
Annual mean variation rate (%)	4.802	1.378	3.551	3.513	9.546	4.497
Mean temperature at 0–0.1 m below ground (°C)	1.327	10.37	3.076	6.582	2.478	5.628
Annual mean variation (°C)	0.237	0.448	0.285	0.465	0.307	0.376
Annual mean variation rate (%)	17.848	4.316	9.261	7.064	12.385	8.257
Mean daily precipitation (mm)	1.170	0.671	0.629	0.252	0.513	0.516
Annual mean variation	0.018	0.028	0.005	0.002	−0.020	0.004
Annual mean variation rate (%)	1.527	4.183	0.788	0.793	−3.969	0.449
Mean VSMC 0–0.1 m below ground (%)	27.524	16.554	24.248	17.991	22.429	20.306
Annual mean variation (%)	0.382	0.244	0.460	0.316	0.487	0.377
Annual mean variation rate (%)	1.389	1.472	1.898	1.758	2.173	1.825

in region 4 was 0.487, the largest of the four regions, as a result of the water conservation effect of the forest cover.

3.3. Synoptic circulation patterns

Strong wind is an important factor in triggering SDSs. In East Asia, SDSs often occur as a result of the southward propagation of cold air from high latitudes, accompanied by strong winds that blow up particles of sand and dust (Kurosaki and Mikami, 2003; Zhang et al., 2005). These particles are then transported toward the east (main direction) or south with the cold anticyclone. The magnitude of the zonal wind component is an important indication of the frequency and intensity of SDSs, whereas the magnitude of the meridional wind component is an important index of the transportation range of the dust. Positive values for the zonal wind component represent the wind from the south whereas negative values represent the wind from the north. Positive values of the meridional wind component represent the wind from the west and negative values represent the wind from the east. The wind direction in region 1 is altered as a result of the topography of the southern Xinjiang basin and therefore we excluded region 1 from the wind analysis.

The zonal and meridional wind components at 850 mbar were analyzed to investigate the near-surface winds. The mean zonal wind components in most the MDIA were negative and the prevailing north wind component dominated in spring from 2007 to 2016 (Fig. 7a). The average mean zonal wind component was −1.026 m/s. The annual mean variation in the zonal wind component in regions 2, 3, and 4 was positive, so that the north wind components had a decreasing trend while the south wind components increased. This means that the strong winds associated with cold air in spring decreased over time, resulting

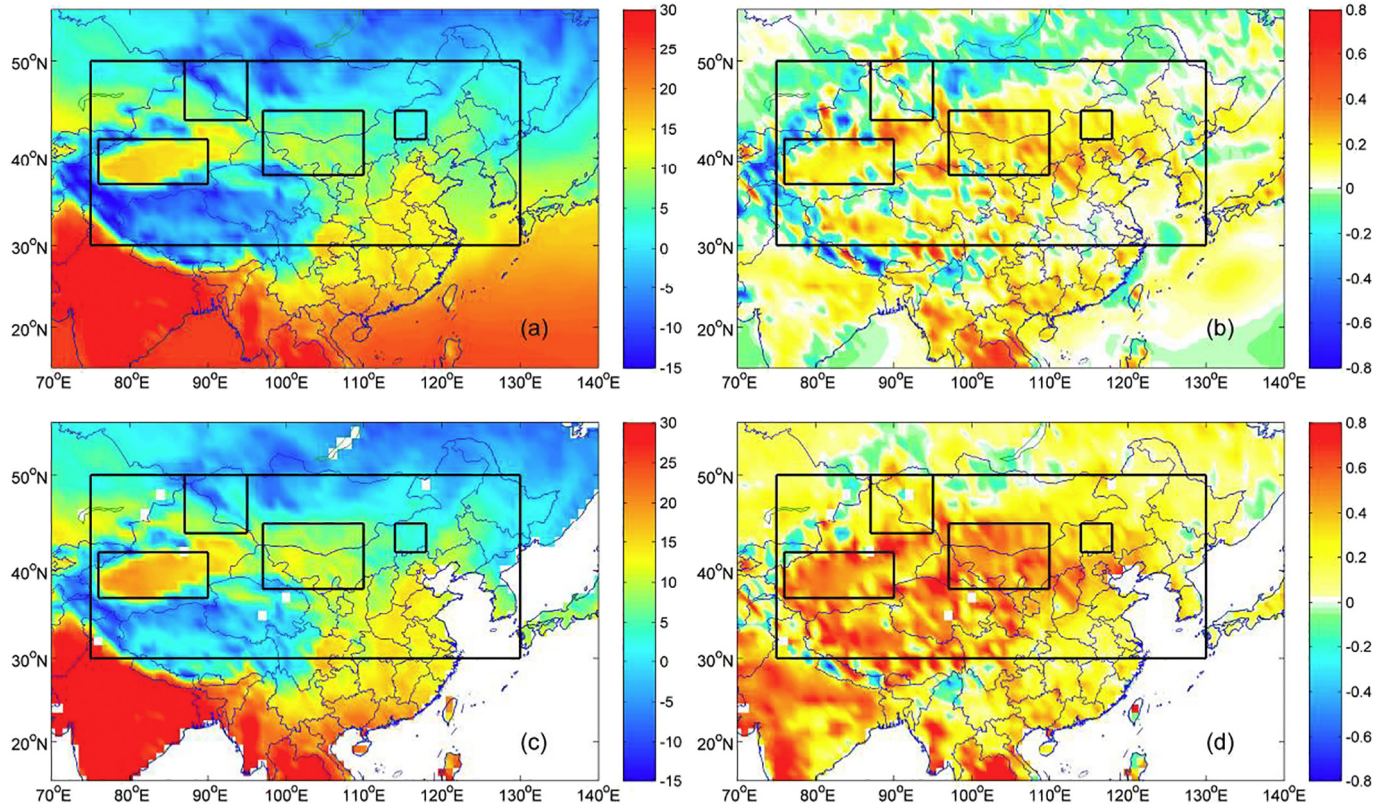

Fig. 4. Mean spring temperature (a) at 2 m height and (c) at 0–0.1 m depth (2007–2016). Annual mean variation of spring temperature (b) at 2 m height and (d) at 0–0.1 m depth (2007–2016). Units: °C.

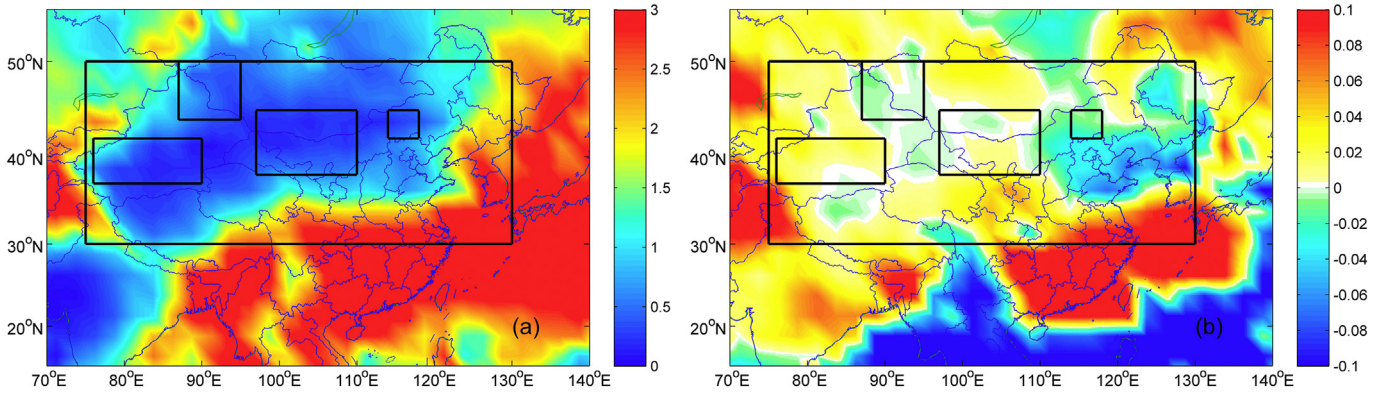

Fig. 5. (a) Mean daily precipitation in spring and (b) annual mean variation in spring precipitation (2007–2016). Units: mm/day.

in a decrease in the number of SDSs. The annual mean variation in the zonal wind component in region 3 was 0.007 m/s per year, much less than in regions 2 and 4 (0.045 and 0.060 m/s, respectively). The mean meridional wind components in MDIA were mostly positive, with a dominant west wind (Fig. 7c). The annual mean variation in the meridional wind component in MDIA was −0.020 m/s per year, indicating a decrease in the west wind component, which does not favor the long distance transport of SDSs to the east (Table 6).

The reduction in the north wind component was accompanied by an increase in the southerly component, indicating that the influx of cold air from the north has decreased and the warm air following the south wind has increased. This favored an increase in temperature. Therefore the reduction in the meridional wind components indirectly decreased the frequency and intensity of SDSs by increasing the temperature of the near-surface layer, which improved the vegetation coverage and surface conditions in the dust source areas.

Strong winds are driven by the pressure gradient force and changes in the pressure at ground level have a large influence on the wind speed in the near-surface layer. Therefore the mean sea-level pressure (MSLP) in East Asia during study period was analyzed to investigate the effects of pressure on winds. The high pressure area between Lake Baikal and Balkhash Lake is the source of cold air influencing East Asia (Fig. 8a). The mean MSLP in the center of this area has a pronounced decreasing trend because the annual mean variation in the MSLP is less than −0.1 hPa per year. The annual mean variation in the MSLP over most of western China and Mongolia was negative, whereas it was mostly positive in eastern China, the Korean Peninsula and Japan (Fig. 8b). Therefore the pressure gradient between the high pressure area and other regions of East Asia decreased each year between 2007 and 2016, resulting in a decrease in the wind velocity to the southeast of the high pressure area, the main source area for dust. The annual mean MSLP variations in regions 1, 2, and 3 were − 0.040, −0.067, and −0.064 hPa per year, indicating that the intensity of the cold anticyclone passing through these areas in spring had a decreasing trend. The annual mean MSLP variations in region 4 were negligible over this time period (Table 6).

There is a small area in western Mongolia where there was an increase in the annual mean MSLP variations, which may have increased the pressure gradient between region 3 and the surrounding area at small scales. This will cause abnormal increase of wind speed in the near-surface layer, resulting in an increasing trend of the surface dust concentration occurred in western Mongolia.

Strong winds that cause SDSs in East Asia are usually caused by an influx of cold air from high latitudes. The polar vortex affects the frequency and intensity of influxes of cold air into the middle to high latitude regions of East Asia. Fig. 9a shows the mean geopotential height at 500 mbar during study period. The polar vortex is a dipole, with one center in northern Asia and the other in Canada. The polar vortex center in north Asia, which deviates from the polar region, causes the progression of cold air in East Asia. The annual mean variation in the geopotential height at 500 mbar around the polar region showed an increasing trend in spring from 2007 to 2016 (Fig. 9b), resulting in a decrease in the intensity of the polar vortex.

The intensity of the polar vortex in spring 2015 was stronger than the climatological mean, which explains the abnormally large number of BSD events in spring 2015. However, the intensity of SDSs events in spring 2015 was weak, which may have been a result of the improvement in surface conditions in the dust source regions. By contrast, in 2013, which had the lowest number of dust storms in the decade 2007–2016, the intensity of the polar vortex was much weaker than the climatological mean.

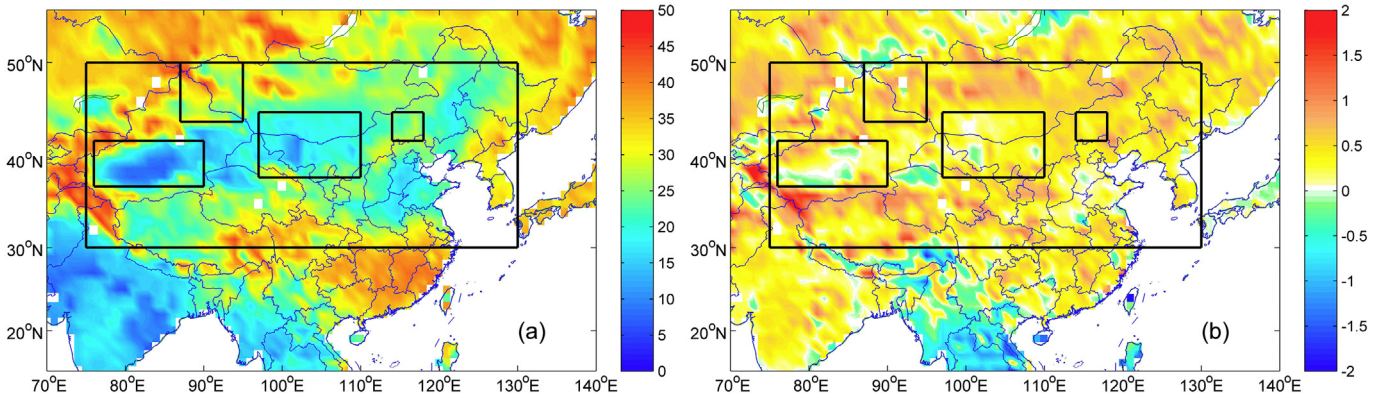

Fig. 6. (a) Mean spring VSMC at 0–0.1 m depth and (b) annual mean variation in the spring VSMC at 0–0.1 m depth (2007–2016). Units: %.

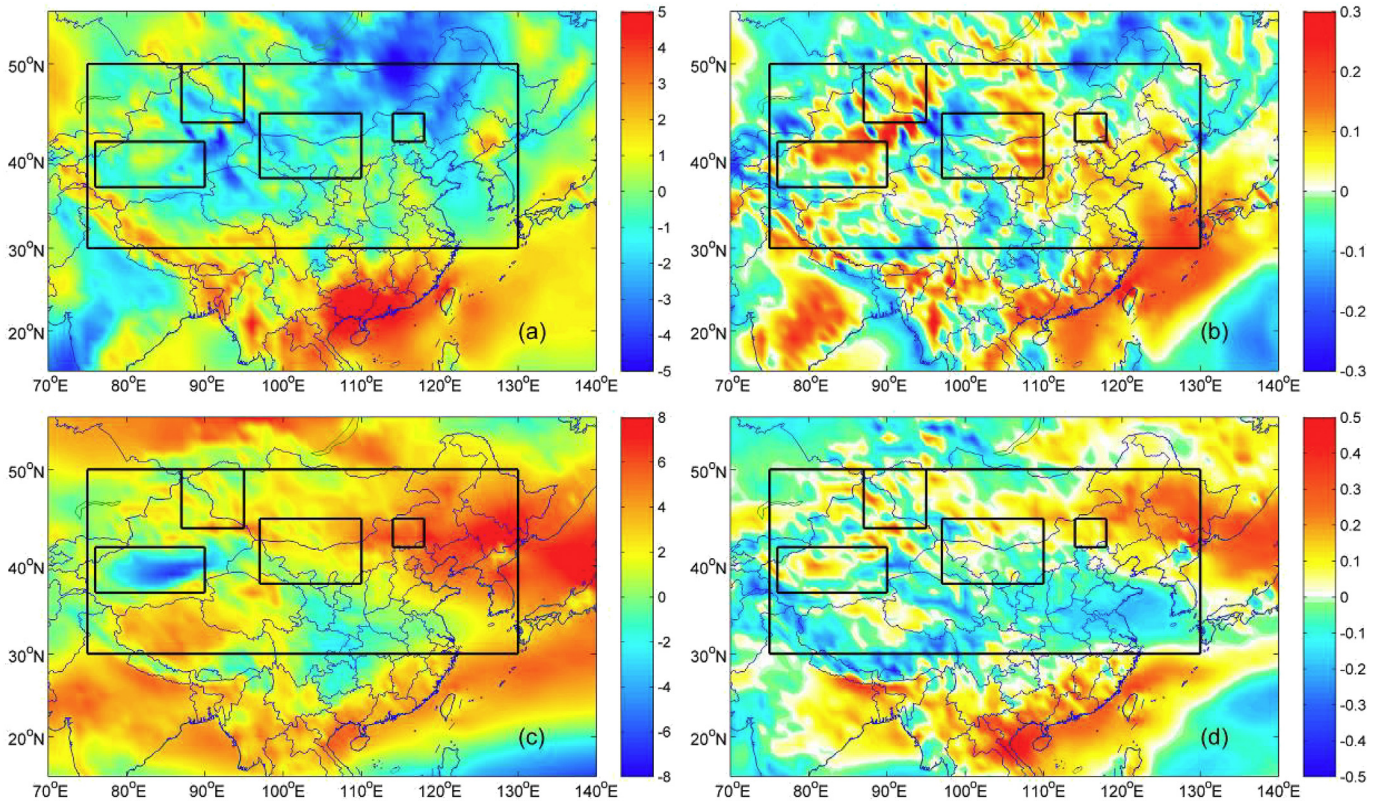

Fig. 7. (a) Mean zonal wind component and (c) radial wind component at 850 mbar in spring from 2007 to 2016. Annual mean variation of (b) the zonal wind component and (d) the meridional wind component in spring from 2007 to 2016. Units: m/s.

4. Conclusions

The following conclusions can be drawn from the results obtained in this study.

(1) The spring SDS events recorded by the CMA from 2007 to 2016 showed decreasing trends in both number and intensity, with 2011 as a clear boundary year. There were five to eight spring SDS events in each of the four years before 2011, but only one or two in each of the six years after 2011. In the same time period, the total number of SDS events decreased from at least ten each year before 2011 to less than ten times per year after 2011, with some exceptions. The SDS events in spring 2007 were the strongest and SDS events occurred most frequently in spring 2010 (15 events). The lowest number of SDS events occurred in spring 2013 (6 events) and their intensity was the weakest.

(2) The distribution of the mean surface dust concentration in spring varied greatly in different regions during 2007 to 2016, particularly in the source areas regions for dust. Most of East Asia was affected by SDSs and the mean surface dust concentration in these regions decreased each year. The decreasing trend of the surface dust concentration was greater in the areas with a high mean surface dust concentration. The overall average annual variation of the surface dust concentration in four dust source regions were − 33.24 μg/m^3 (−11.75%) per year. The decrease was greatest in central Inner Mongolia, where the mean surface dust concentration decreased on average by 45.05 μg/m^3 (16.25%).

(3) Based on the NDVI, the vegetation coverage improved and spring dust emissions were suppressed in and around the dust source regions during 2007 to 2016. The mean temperature at 2 m height and at 0–0.1 m depth level in the MDIA showed an increasing trend and the amount of precipitation also increased over time. The VSMC at 0–0.1 m depth level in most parts of MDIA increased each year. These conditions are favorable for plant growth, which may reduce the intensity and frequency of SDSs. Artificial afforestation has also played an important part in the improvement of vegetation coverage. Although the condition of vegetation coverage because better and better on the edge of deserts, little were changed in the desert interiors. That's

Table 6
Mean zonal and meridional wind components, MSLP and annual mean variations (rates) in major regions in spring from 2007 to 2016.

	MDIA	Region 1	Region 2	Region 3	Region 4	Average (regions 1–4)
Zonal wind component at 850 mbar (m/s)	−0.540	−0.790	−0.921	−1.027	−1.364	−1.026
Annual mean variation (m/s)	−0.004	0.034	0.045	0.007	0.060	0.036
Annual mean variation rate (%)	0.702	−4.253	−4.911	−0.634	−4.392	−3.547
Meridional wind component at 850 mbar (m/s)	2.720	−1.341	1.200	2.053	4.584	1.624
Annual mean variation V (m/s)	−0.020	−0.012	0.028	−0.004	0.086	0.024
Annual mean variation rate (%)	−0.717	0.891	2.300	−0.211	1.875	1.214
MSLP (hPa)	1004.740	1002.470	1006.822	1004.203	1003.704	1004.300
Annual mean variation (hPa)	−0.024	−0.040	−0.067	−0.064	0.001	−0.043
Annual mean variation rate (%)	−0.002	−0.004	−0.007	−0.006	0.000	−0.004

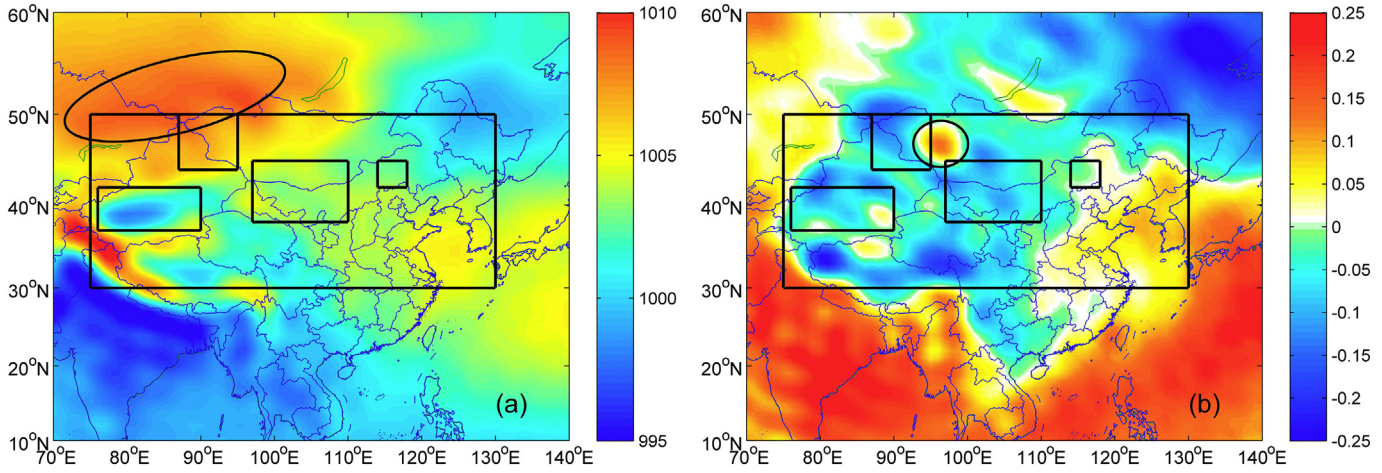

Fig. 8. (a) Mean MSLP and (b) annual mean variation in spring from 2007 to 2016. Units: hPa.

because the measures to prevent and control desertification are unable to change the condition of vegetation coverage in the interior of deserts, including the Gobi Desert.

(4) The strong winds that blow up sand and dust particles are usually accompanied by an influx of cold air from high latitudes. The north wind components showed a decreasing trend, resulting

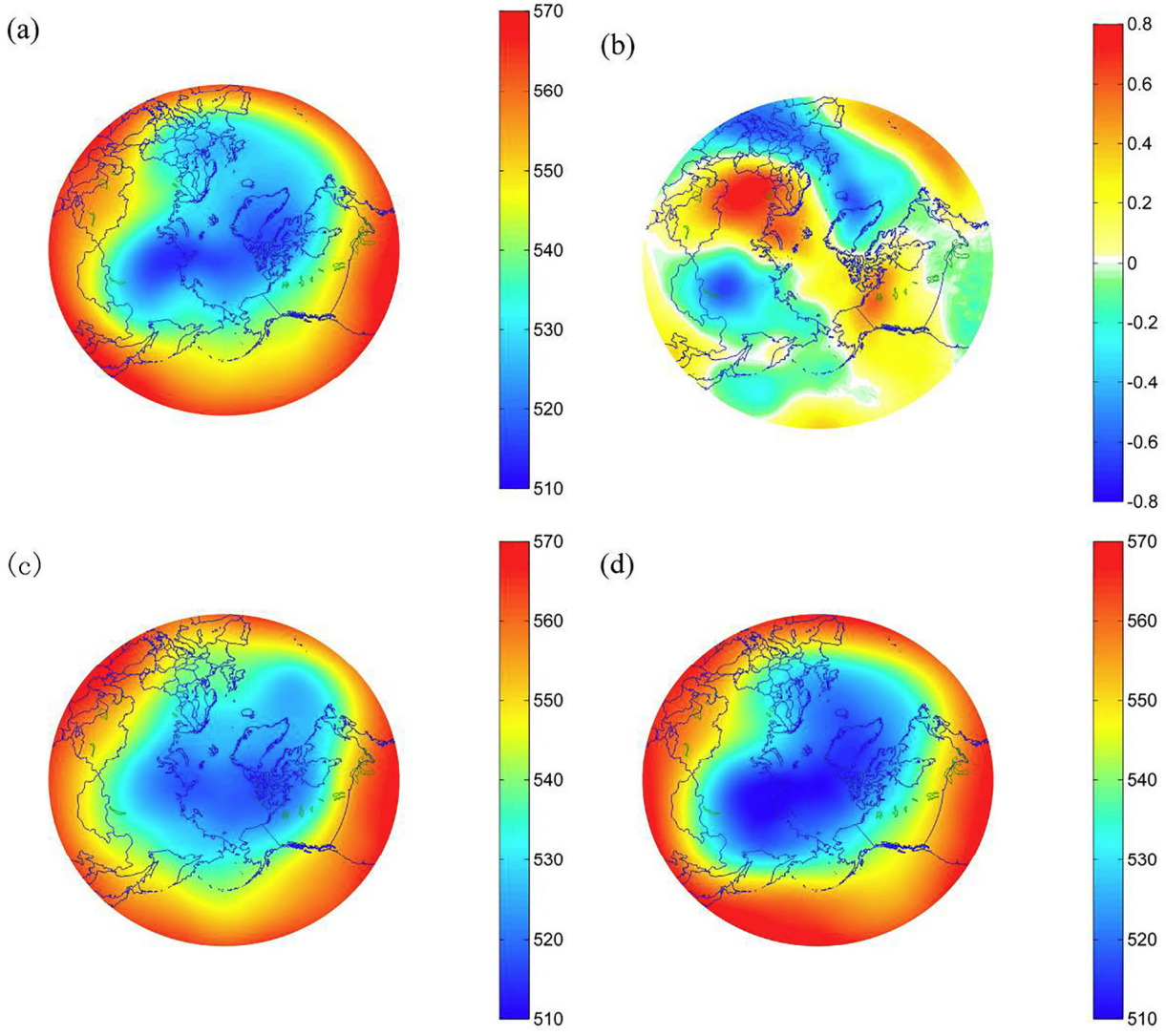

Fig. 9. (a) Mean geopotential height at 500 mbar and (b) annual mean variation in spring (2007–2016). Mean geopotential height at 500 mbar in (c) spring 2013 and (d) spring 2015. Units: gpm.

in a decrease in the number of SDSs, while the observed decrease in the west wind component was not conducive to the long distance transmission of SDSs to the east. The MSLP gradient between the high pressure area in northwest Asia and in East Asia decreasing showed an annual decrease over the decade, which resulted in a decrease in wind velocity in the main source area for dust. The decreased intensity of the polar vortex, which affects the frequency and intensity of the influx of cold air into East Asia, was closely related to the decrease in the intensity and frequency of SDSs. As the decrease of wind speed could influence the SDSs both on the edge of deserts and in the desert interiors, it played a key role in the decadal decrease of SDSs.

Acknowledgments

This work was supported by grants from the National Key R & D Program Pilot Projects of China (2016YFA0601901, 2016YFC0203301), National Natural Science Foundation of China (41590874 & 41375153), CAMS Basis Research Project (2017Z11, 2016Z001 & 2014R17), the Climate Change Special Fund of CMA (CCSF201504).

References

Adler, R.F., Huffman, G.J., Chang, A., Ferraro, R., Xie, P., Janowiak, J., Rudolf, B., Schneider, U., Curtis, S., Bolvin, D., Gruber, A., Susskind, J., Arkin, P., 2003. The version 2 Global Precipitation Climatology Project (GPCP) monthly precipitation analysis. J. Hydrometeorol. 4:1147–1167. https://www.esrl.noaa.gov/psd/data/gridded/data.gpcp.html.

Bi, J., Shi, J., Xie, Y., Liu, Y., Takamura, T., Khatri, P., 2014. Dust aerosol characteristics and shortwave radiative impact at a Gobi Desert of Northwest China during the spring of 2012. J. Meteorol. Soc. Jpn. 92, 33–56 Ser. II..

Che, H., Zhang, X., Shi, G., Li, Y., Zhao, J., Qu, W., et al., 2005. Aerosol optical characteristics in Mu Us desert under weather conditions of dust storm and haze. China Powder Sci. Technol. 11, 4–7.

Che, H., Zhang, X., Li, Y., Zhou, Z., Chen, Z., 2006. Relationship between horizontal extinction coefficient and PM10 concentration in Xi'an, China, during 1980–2002. China Particuol. 4, 327–329.

Che, H., Wang, Y., Sun, J., 2011. Aerosol optical properties at Mt. Waliguan observatory, China. Atmos. Environ. 45, 6004–6009.

Che, H., Wang, Y., Sun, J., Zhang, X., Zhang, X., Guo, J., 2013. Variation of aerosol optical properties over the Taklimakan Desert in China. Aerosol Air Qual. Res. 13, 777–785.

Che, H., Zhao, H., Wu, Y., Xia, X., Zhu, J., Dubovik, O., et al., 2015. Application of aerosol optical properties to estimate aerosol type from ground-based remote sensing observation at urban area of northeastern China. J. Atmos. Sol. Terr. Phys. 132, 37–47.

Chen, S., Huang, J., Kang, L., Wang, H., Ma, X., He, Y., et al., 2017a. Emission, transport, and radiative effects of mineral dust from the Taklimakan and Gobi deserts: comparison of measurements and model results. Atmos. Chem. Phys. 17, 2401.

Chen, S., Huang, J., Qian, Y., Zhao, C., Kang, L., Yang, B., et al., 2017b. An overview of mineral dust modeling over East Asia. J. Meteorol. Res. 31, 633–653.

China Meteorological Administration (CMA), 2006. Grade of sand and dust storm weather. (GB/T 20480–2006). in Chinese.

Chun, Y., Boo, K.O., Kim, J., Park, S.U., Lee, M., 2001. Synopsis, transport, and physical characteristics of Asian dust in Korea. J. Geophys. Res. Atmos. 106, 18461–18469.

Didan, K., 2015. MOD13A3 MODIS/Terra Vegetation Indices Monthly L3 Global 1km SIN Grid V006 [Data set]. NASA EOSDIS LP DAAC. https://doi.org/10.5067/MODIS/MOD13A3.006.

Fan, K., Xie, Z., Wang, H., Xu, Z., Liu, J., 2017. Frequency of spring dust weather in North China linked to sea ice variability in the Barents Sea. Clim. Dyn. 1–12.

Gong, S., Zhang, X., 2008. CUACE/Dust–an integrated system of observation and modeling systems for operational dust forecasting in Asia. Atmos. Chem. Phys. 8, 2333–2340.

Gong, S., Zhang, X., Zhao, T., Zhang, X., Barrie, L., McKendry, I., et al., 2006. A simulated climatology of Asian dust aerosol and its trans-Pacific transport. Part II: interannual variability and climate connections. J. Clim. 19, 104–122.

Gong, D.Y., Mao, R., Shi, P.J., Fan, Y.D., 2007. Correlation between East Asian dust storm frequency and PNA. Geophys. Res. Lett. 34.

Gottfried, M., Pauli, H., Futschik, A., Akhalkatsi, M., Barančok, P., Alonso, J.L.B., et al., 2012. Continent-wide response of mountain vegetation to climate change. Nat. Clim. Chang. 2, 111.

Grousset, F.E., Ginoux, P., Bory, A., Biscaye, P.E., 2003. Case study of a Chinese dust plume reaching the French Alps. Geophys. Res. Lett. 30.

Guan, Q., Yang, J., Zhao, S., Pan, B., Liu, C., Zhang, D., et al., 2015. Climatological analysis of dust storms in the area surrounding the Tengger Desert during 1960–2007. Clim. Dyn. 45, 903–913.

Huang, J., Wang, T., Wang, W., Li, Z., Yan, H., 2014. Climate effects of dust aerosols over East Asian arid and semiarid regions. J. Geophys. Res. Atmos. 119.

Kelly, A.E., Goulden, M.L., 2008. Rapid shifts in plant distribution with recent climate change. Proc. Natl. Acad. Sci. 105, 11823–11826.

Kim, K.W., Kim, Y.J., Oh, S.J., 2001. Visibility impairment during Yellow Sand periods in the urban atmosphere of Kwangju, Korea. Atmos. Environ. 35, 5157–5167.

Kim, D., Chin, M., Bian, H., Tan, Q., Brown, M.E., Zheng, T., et al., 2013. The effect of the dynamic surface bareness on dust source function, emission, and distribution. J. Geophys. Res. Atmos. 118, 871–886.

Kurosaki, Y., Mikami, M., 2003. Recent frequent dust events and their relation to surface wind in East Asia. Geophys. Res. Lett. 30.

Lee, E.-H., Sohn, B.-J., 2011. Recent increasing trend in dust frequency over Mongolia and Inner Mongolia regions and its association with climate and surface condition change. Atmos. Environ. 45, 4611–4616.

Li, J., Wang, Z., Zhuang, G., Luo, G., Sun, Y., Wang, Q., 2012. Mixing of Asian mineral dust with anthropogenic pollutants over East Asia: a model case study of a superduststorm in March 2010. Atmos. Chem. Phys. 12, 7591–7607.

Littmann, T., 1991. Dust storm frequency in Asia: climatic control and variability. Int. J. Climatol. 11, 393–412.

Liu, X., Yin, Z.Y., Zhang, X., Yang, X., 2004. Analyses of the spring dust storm frequency of northern China in relation to antecedent and concurrent wind, precipitation, vegetation, and soil moisture conditions. J. Geophys. Res. Atmos. 109.

Martínez-Garcia, A., Rosell-Melé, A., Jaccard, S.L., Geibert, W., Sigman, D.M., Haug, G.H., 2011. Southern Ocean dust-climate coupling over the past four million years. Nature 476, 312.

Meng, Z., Lu, B., 2007. Dust events as a risk factor for daily hospitalization for respiratory and cardiovascular diseases in Minqin, China. Atmos. Environ. 41, 7048–7058.

Mikami, M., Aoki, T., Ishizuka, M., YABUM, S., Yamada, Y., GAO, W., et al., 2005. Observation of number concentration of desert aerosols in the south of the Taklimakan Desert, China. J. Meteorol. Soc. Jpn. 83, 31–43 Ser. II.

Miller, J., Barlage, M., Zeng, X., Wei, H., Mitchell, K., Tarpley, D., 2006. Sensitivity of the NCEP/Noah land surface model to the MODIS green vegetation fraction data set. Geophys. Res. Lett. 33.

Mukai, M., Nakajima, T., Takemura, T., 2004. A study of long-term trends in mineral dust aerosol distributions in Asia using a general circulation model. J. Geophys. Res. Atmos. 109.

National Centers for Environmental Prediction (NCEP)/National Weather Service/NOAA/U.S. Department of Commerce, 2000. NCEP FNL Operational Model Global Tropospheric Analyses, Continuing From July 1999. https://doi.org/10.5065/D6M043C6.

Natsagdorj, L., Jugder, D., Chung, Y., 2003. Analysis of dust storms observed in Mongolia during 1937–1999. Atmos. Environ. 37, 1401–1411.

Peng, S., Piao, S., Zeng, Z., Ciais, P., Zhou, L., Li, L.Z., et al., 2014. Afforestation in China cools local land surface temperature. Proc. Natl. Acad. Sci. 111, 2915–2919.

Qian, W., Quan, L., Shi, S., 2002. Variations of the dust storm in China and its climatic control. J. Clim. 15, 1216–1229.

Qu, J., Hao, X., Kafatos, M., Wang, L., 2006. Asian dust storm monitoring combining Terra and Aqua MODIS SRB measurements. IEEE Geosci. Remote Sens. Lett. 3, 484–486.

Seinfeld, J.H., Carmichael, G.R., Arimoto, R., Conant, W.C., Brechtel, F.J., Bates, T.S., et al., 2004. ACE-ASIA: regional climatic and atmospheric chemical effects of Asian dust and pollution. Bull. Am. Meteorol. Soc. 85, 367–380.

Song, H., Zhang, K., Piao, S., Wan, S., 2016. Spatial and temporal variations of spring dust emissions in northern China over the last 30 years. Atmos. Environ. 126, 117–127.

Sun, J., Zhang, M., Liu, T., 2001. Spatial and temporal characteristics of dust storms in China and its surrounding regions, 1960–1999: relations to source area and climate. J. Geophys. Res. Atmos. 106, 10325–10333.

Tam, W.W., Wong, T.W., Wong, A.H., Hui, D.S., 2012. Effect of dust storm events on daily emergency admissions for respiratory diseases. Respirology 17, 143–148.

Tan, M., Li, X., 2015. Does the Green Great Wall effectively decrease dust storm intensity in China? A study based on NOAA NDVI and weather station data. Land Use Policy 43, 42–47.

Tan, S.-C., Shi, G.-Y., Wang, H., 2012. Long-range transport of spring dust storms in Inner Mongolia and impact on the China seas. Atmos. Environ. 46, 299–308.

Tan, S.-C., Yao, X., Gao, H.-W., Shi, G.-Y., Yue, X., 2013. Variability in the correlation between Asian dust storms and chlorophyll a concentration from the north to equatorial Pacific. PLoS One 8, e57656.

Tegen, I., 2003. Modeling the mineral dust aerosol cycle in the climate system. Quat. Sci. Rev. 22, 1821–1834.

Wang, X., Zhou, Z., Dong, Z., 2006. Control of dust emissions by geomorphic conditions, wind environments and land use in northern China: an examination based on dust storm frequency from 1960 to 2003. Geomorphology 81, 292–308.

Wang, X., Huang, J., Ji, M., Higuchi, K., 2008a. Variability of East Asia dust events and their long-term trend. Atmos. Environ. 42, 3156–3165.

Wang, Y., Zhang, X., Gong, S., Zhou, C., Hu, X., Liu, H., et al., 2008b. Surface observation of sand and dust storm in East Asia and its application in CUACE/Dust. Atmos. Chem. Phys. 8, 545–553.

Wang, Y., Che, H., Ma, J., Wang, Q., Shi, G., Chen, H., et al., 2009. Aerosol radiative forcing under clear, hazy, foggy, and dusty weather conditions over Beijing, China. Geophys. Res. Lett. 36.

Wang, X., Liu, J., Che, H., Ji, F., Liu, J., 2018. Spatial and temporal evolution of natural and anthropogenic dust events over northern China. Sci. Rep. 8, 2141.

Xu, D., Qu, J.J., Niu, S., Hao, X., 2011. Sand and dust storm detection over desert regions in China with MODIS measurements. Int. J. Remote Sens. 32, 9365–9373.

Yang, B., Bräuning, A., Zhang, Z., Dong, Z., Esper, J., 2007. Dust storm frequency and its relation to climate changes in Northern China during the past 1000 years. Atmos. Environ. 41, 9288–9299.

Yang, Y., Hou, Q., Zhou, C., Liu, H., Wang, Y., Niu, T., 2008. Sand/dust storm processes in Northeast Asia and associated large-scale circulations. Atmos. Chem. Phys. 8, 25–33.

Yu, R., Li, J., Chen, H., 2009. Diurnal variation of surface wind over central eastern China. Clim. Dyn. 33, 1089.

Yuan, W., Zhang, J., 2006. High correlations between Asian dust events and biological productivity in the western North Pacific. Geophys. Res. Lett. 33.
Zhang, X., Arimoto, R., An, Z.S., 1997. Dust emission from Chinese desert sources linked to variations in atmospheric circulation. J. Geophys. Res. Atmos. 102, 28041–28047.
Zhang, X., Arimoto, R., Zhu, G., Chen, T., Zhang, G., 1998. Concentration, size-distribution and deposition of mineral aerosol over Chinese desert regions. Tellus Ser. B Chem. Phys. Meteorol. 50, 317–330.
Zhang, X., Gong, S., Zhao, T., Arimoto, R., Wang, Y., Zhou, Z., 2003a. Sources of Asian dust and role of climate change versus desertification in Asian dust emission. Geophys. Res. Lett. 30.
Zhang, X., Gong, S., Shen, Z., Mei, F., Xi, X., Liu, L., et al., 2003b. Characterization of soil dust distributions in China and its transport during ACE-Asia 1. Net work measurements. J. Geophys. Res. 108, 4261.
Zhang, J., Dong, W., Fu, C., 2005. Impact of land surface degradation in northern China and southern Mongolia on regional climate. Chin. Sci. Bull. 50, 75–81.
Zhang, B., Tsunekawa, A., Tsubo, M., 2008. Contributions of sandy lands and stony deserts to long-distance dust emission in China and Mongolia during 2000–2006. Glob. Planet. Chang. 60, 487–504.
Zhao, C., Dabu, X., Li, Y., 2004. Relationship between climatic factors and dust storm frequency in Inner Mongolia of China. Geophys. Res. Lett. 31.
Zhou, Z., Wang, X., 2002. Analysis of the severe group dust storms in eastern part of Northwest China. J. Geogr. Sci. 12, 357–362.
Zhou, C., Gong, S., Zhang, X., Wang, Y., Niu, T., Liu, H., et al., 2008. Development and evaluation of an operational SDS forecasting system for East Asia: CUACE/Dust. Atmos. Chem. Phys. 8, 787–798.